Principles of remote sensing of atmospheric parameters from space February 1998

By **R. Rizzi and updated by R. Saunders**

European Centre for Medium-Range Weather Forecasts, Shinfield Park, Reading RG2 9AX, U.K.

Table of contents

1. INTRODUCTION

The interaction of electromagnetic radiation with matter modifies to some extent the incident wave. The medium therefore produces a signature in the amplitude, phase or spectral composition which depends on composition and structure of the medium. The basic principle associated with remote sensing of the atmospheric temperature and humidity structure involves the interpretation of radiometric measurements of electromagnetic radiation in specific spectral intervals which are sensitive to some physical aspects of the medium. More specifically, at any wavenum-

ber (or wavelength) in the infrared or microwave regions where an atmospheric constituent absorbs radiation, it also emits thermal radiation according to Kirchhoff's Law. Since the radiance leaving the atmosphere is a function of the distribution of the emitting gases and of temperature throughout the atmosphere, measurements of radiance contain some information on both these quantities.

These lectures will start with an introduction to the basic radiometric quantities and laws to be used, then will derive and discuss the equation of radiative transfer for an absorbing and emitting medium. No scattering is included so the results will be applicable only to situations in which scattering phenomena play a secondary role, as is the case for the energy transfer in the clear atmosphere in the infrared and at microwave frequencies, provided no clouds are involved in which precipitation is taking place nor ice phase is present. The concepts outlined below are described in more detail in Goody and Yung (1989**)** to which the interested reader is referred.

2. Absorption and transmission of monochromatic radiation

Referring to Fig. 1 , radiance is the amount of energy crossing, in a time interval $\mathrm{d}t$ and in the wavenumber interval ν to $\nu + \mathrm{d}\nu$, a differential area $\mathrm{d}A$ at an angle θ to the normal to $\mathrm{d}A$, the beam being confined to a solid angle $\mathrm{d}\Omega$. In other words

$$L_\nu = \frac{\mathrm{d}E_\nu}{\cos\theta \ \mathrm{d}A \ \mathrm{d}t \ \mathrm{d}\Omega \ \mathrm{d}\nu} \tag{1}$$

and the unit is $\mathrm{W(m^2\ sr\ cm^{-1})^{-1}}$.

Sometimes different units are used, like $\mathrm{mW(m^2\ sr\ cm^{-1})^{-1}}$ whose numerical values are the same as in CGS units. Radiance can also be defined for a unit wavelength λ or frequency interval ν (in units of inverse centimetres) the relation among these quantities being

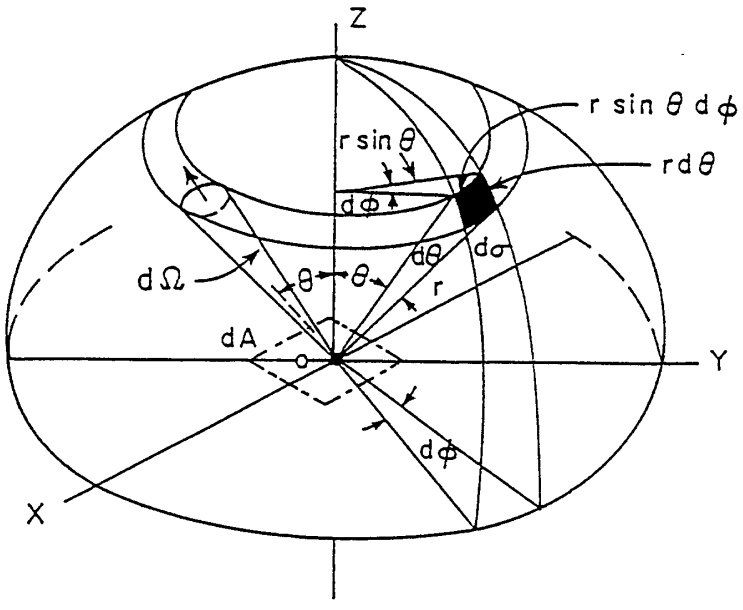

Figure 1. Illustrating a pencil of radiation through an element of area $\mathrm{d}A$ in direction confined to an element of solid angle $\mathrm{d}\Omega$ (figure taken from Liou, 1980).

$$\lambda = \frac{c}{\tilde{\nu}} = \frac{1}{\nu}$$

where c is the speed of light in vacuum and $\tilde{\nu}$ is frequency (in units of Hz). Spectroscopists have adopted the wavenumber as the normal unit for frequency and this is used throughout this report. However at microwave frequencies the true frequency (in GHz) is often employed.

Whenever a beam of monochromatic radiation, whose radiance is L_ν enters an absorbing medium (see Fig. 2), the fractional decrease experienced is:

$$\frac{\mathrm{d}L_\nu}{L_\nu} = -k_\nu \rho \, \mathrm{d}x \tag{2}$$

where $\rho = \rho(x)$ is the density of the medium at x and k_ν is a proportionality factor called the (spectral) absorption coefficient. Integrating Eq. (2) between 0 and x yields

$$L_\nu(x) = L_\nu(0)\exp\left(-\int_0^x k_\nu \rho \, \mathrm{d}x\right) \tag{3}$$

where $L_\nu(0)$ is the boundary value, i.e. the radiance entering the medium at $x = 0$. The ratio $L_\nu(x)/L_\nu(0)$ is called the (spectral) transmittance of the Black Body radiation medium.and $-\int_0^x k_\nu \rho \, \mathrm{d}x$ is the optical depth. An example of the use of Eq. (3) is the modelling of attenuation of the solar direct beam due to atmospheric constituents. The real problem lies, as always, in the knowledge of k_ν the absorption coefficient of the gases.

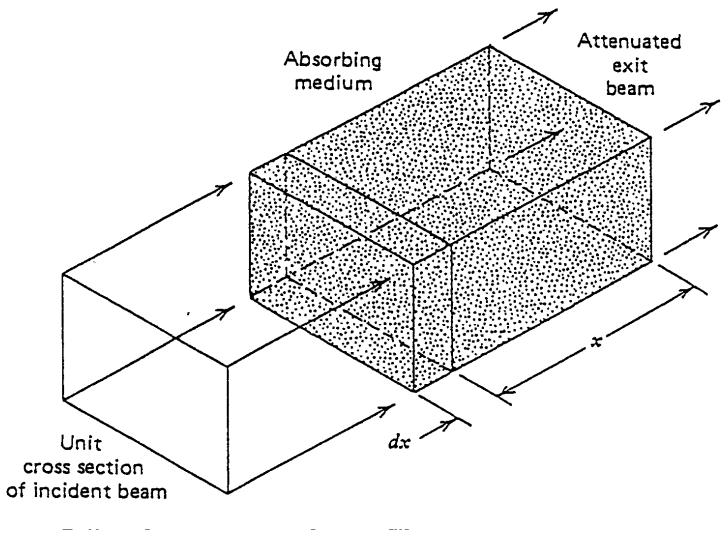

Figure 2. (figure taken from McCartney, 1983).

3. Black Body radiation

To explain the spectral distribution of radiance emitted by solid bodies, Planck found that the radiance per unit frequency emitted by a *blackbody* at temperature T is expressed by

$$B_\nu(T) = \frac{2h\nu^3 c}{\exp\left(\frac{h\nu c}{\kappa T}\right) - 1} \tag{4}$$

where h is Planck's constant and κ is Boltzmann's constant. An equivalent formula in terms of radiance per unit wavelength is

$$B_\lambda(T) = \frac{2hc^2}{\lambda^5\left[\exp\left(\frac{hc}{\kappa\lambda T}\right) - 1\right]} \tag{5}$$

The above two equations can be simplified by defining:

$$C_1 = 2\pi hc^2$$

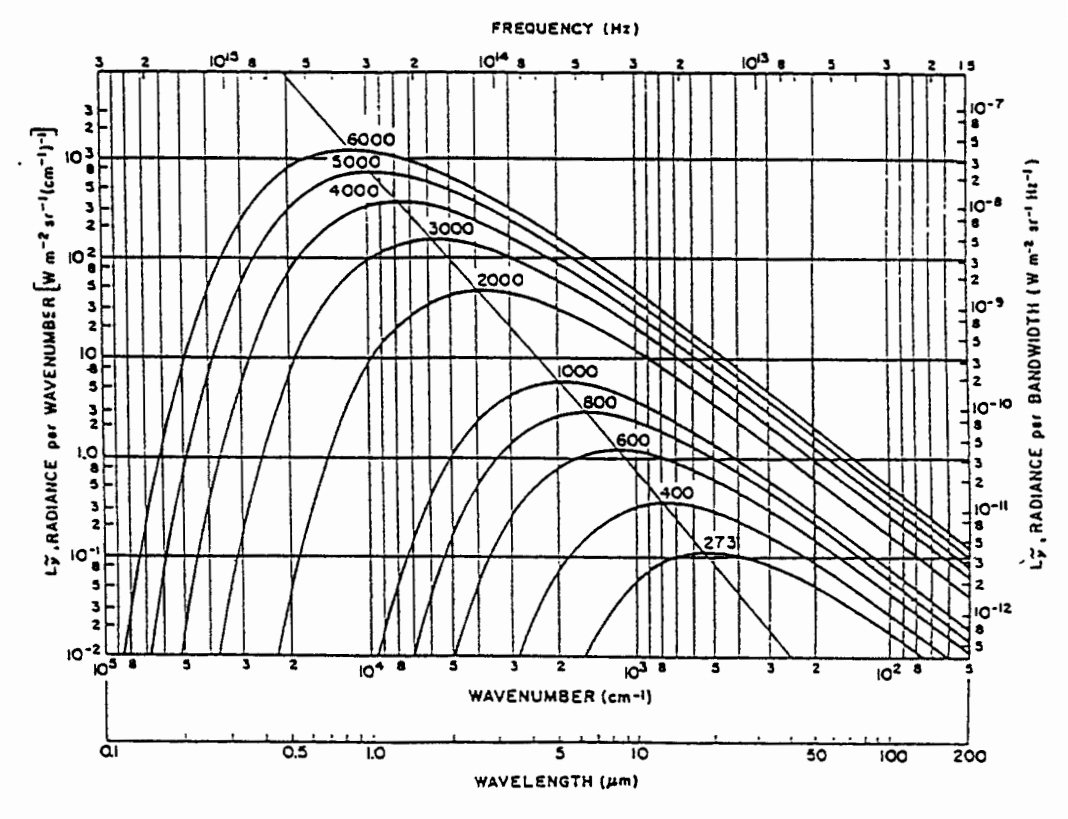

Figure 3. Spectral radiance of a blackbody, per unit wavenumber interval and per unit frequency interval, at the Kelvin temperatures shown in each curve (taken from Valley, 1965).

$$C_2 = \frac{hc}{\kappa}$$

as the first and second radiation constant respectively. Figures 3 and 4 show curves of $B_\nu(T)$ versus wave number and $B_\lambda(T)$ versus wavelength.

Equation (4) implies that, as long as a cavity is in thermodynamic equilibrium (TE) at a given temperature, the spectral distribution of radiance emitted by the cavity depends only on its temperature, whatever spectral distribution of radiance is entering the cavity. This is because quanta entering a perfect black cavity undergo a succession of internal reflections and absorptions until all the energy is absorbed within the cavity.

4. Emissivity, Kirchhoff Law and Local Thermodynamical Equilibrium.

In general a medium that absorbs radiation may also emit radiation at the same wavenumber. If we enclose the volume of gas in Fig. 2 in a black box in thermodynamic (TE) with the gas, the temperature T of its walls being the same as that of the gas, then the radiance emitted from the walls of the box in all directions will be $B_\nu(T)$ and the amount of energy absorbed in the any direction (say x for convenience) by a layer dx deep of gas is $B_\nu(T)k_\nu\rho\mathrm{d}x$.

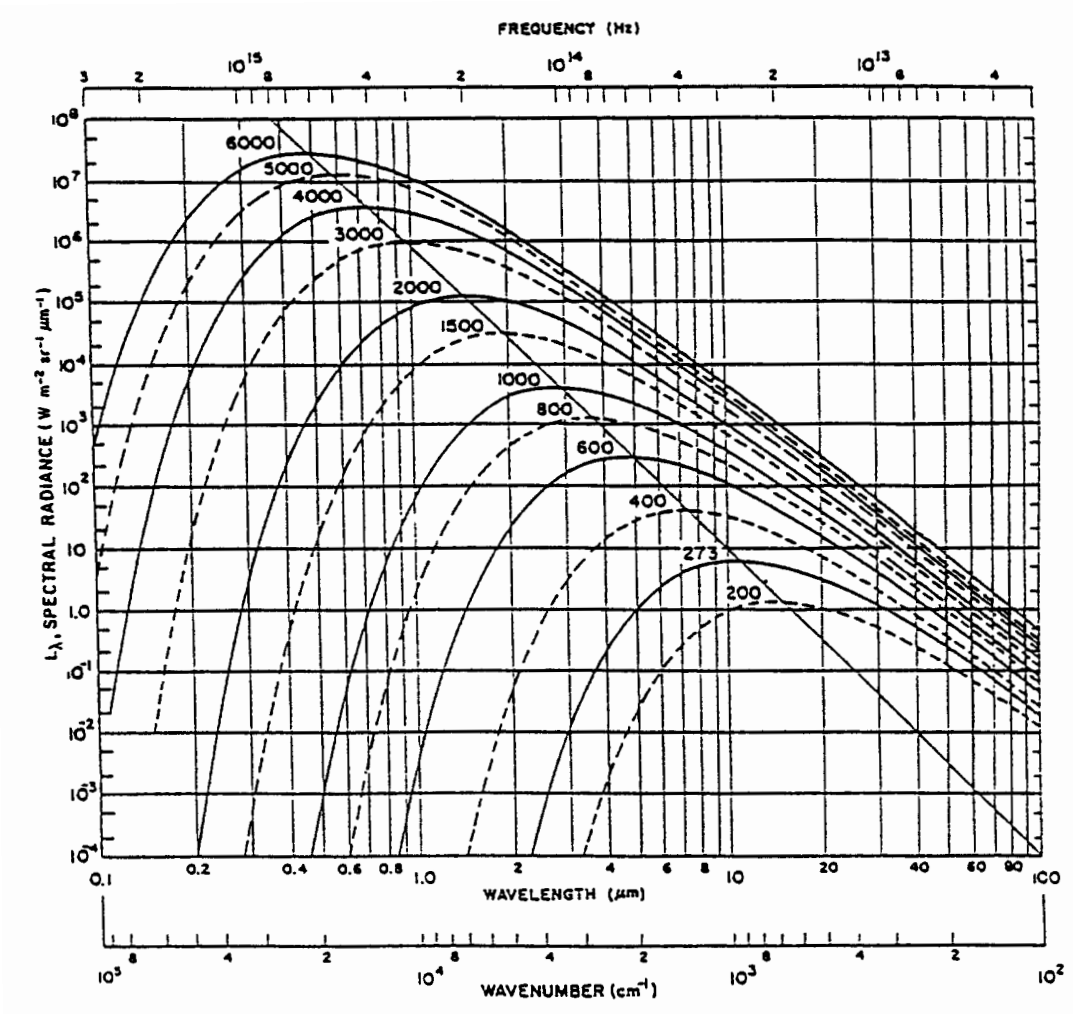

Figure 4. Spectral radiance of a blackbody, per unit wavelength interval, at the Kelvin temperatures shown in each curve (taken from Valley, 1965).

The same amount of gas will emit in the x-direction an amount of energy $B_\nu(T)\varepsilon_\nu\rho\mathrm{d}x$ where ε_ν is a proportionality constant called the (spectral) emissivity of the gas. Now the amount of emitted energy must be equal to the amount of energy absorbed in the same direction, for equilibrium conditions; otherwise equilibrium would not be

possible and the second law of thermodynamics would be violated. This in turn implies the equality of the absorption and emission coefficients $k_\nu = \varepsilon_\nu$ when TE is achieved, which is a way of stating Kirchhoff's Law.

The radiation field of the earth atmosphere, as a whole, is not in TE. However, below about 40 to 60 km, a volume of gas behaves approximately as a black cavity so that the emission from the volume is dependent only on its temperature, whatever the spectral distribution of radiance entering the volume from outside may be. In fact, as soon as a molecule absorbs a quantum of energy, some is lost by collisional exchange with nearby molecules, before emission takes place. These collision exchanges spread the energy of the initial quantum throughout the volume of air. When emission finally occurs, it takes place from an upper energy level which is lower than the level reached after the initial absorption. When the mean time between collisions (relaxation time) is much smaller than the time interval between the initial absorption and final emission (natural lifetime), then a single kinetic temperature characterizes, to a good approximation, the gas. This (lucky) circumstance is denoted by the term Local Thermodynamic Equilibrium. At STP the ratio of relaxation time to natural lifetime is about 10^{-10} for a rotational transition and $10^{-5} \times 10^{-4}$ for a vibrational transition.

5. The Equation for Radiative Transfer

Consider the volume of gas in Fig. 2 in which emission as well as absorption now takes place, but not scattering. The equation of energy transfer can be written, for monochromatic radiation,

$$\mathrm{d}L_\nu = -L_\nu k_\nu \rho \, \mathrm{d}x + J_\nu \rho \, \mathrm{d}x$$

where the x-direction is the direction of propagation of the incident wave, x can now take values from 0 to a. The first term on the right-hand side is the effect of absorption within $\mathrm{d}x$, and J_ν is the source of radiant emission within $\mathrm{d}x$. We are interested in computing the value of radiance at $x = a$. Dropping for simplicity the subscript ν and applying the Kirchhoff law we get:

$$\frac{1}{k\rho}\frac{\mathrm{d}L(x)}{\mathrm{d}x} = -L(x) + B(T_x) \tag{6}$$

where T_x is the temperature of the gas at x. We define the monochromatic optical depth $\sigma(x, a)$ of the medium between points x and a as

$$\sigma(x, a) = \int_x^a k\rho \, \mathrm{d}x' \tag{7}$$

$$\mathrm{d}\sigma(x, a) = \frac{\mathrm{d}\sigma(x, a)}{\mathrm{d}x}\mathrm{d}x = -k\rho \, \mathrm{d}x$$

Equation (6) can then be written

$$-\frac{\mathrm{d}L(x)}{\mathrm{d}\sigma(x, a)} = -L(x) + B(T_x) \tag{8}$$

Noting that

$$\mathrm{d}[L\exp(-\sigma(x, a))] = \mathrm{d}L \, \exp(-\sigma(x, a)) - L \, \mathrm{d}\sigma \, \exp(-\sigma(x, a))$$

we can multiply Eq. (8) by $\exp[-\sigma(x, a)]$ and then integrate the resultant equation between 0 and a

$$-\int_0^a \mathrm{d}[L\exp(-\sigma(x,a))] = \int_0^a B(T_x)\exp(-\sigma(x,a))\ \mathrm{d}\sigma(x,a)$$

to obtain finally

$$L_\nu(a) = L_\nu(0)\exp(-\int_0^a k_\nu\rho\ \mathrm{d}x) + \int_0^a k_\nu\rho B_\nu(T_x)\exp(-\int_x^a k_\nu\rho\ \mathrm{d}x)\mathrm{d}x \tag{9}$$

The first term on right-hand side of (9) is analogous to the one in Eq. (3) and represents the radiance at the boundary multiplied by the transmittance from the boundary up to a. The second term is the contribution due to emission from the medium in the direction of the incident wave. Each slab $\mathrm{d}x$ around a generic point x radiates depending on the amount of gas ($\rho(x)$) on its emissivity ($= k_\nu$) and on its temperature. The energy is depleted in its way from x to a by a factor given by the transmittance from x to a

$$\tau_\nu(x, a) = \exp(-\int_x^a k_\nu\rho\ \mathrm{d}x)$$

A similar equation is obtained when computing the radiance emitted by the atmosphere in any upward direction toward space. Denoting by z the zenith axis (z_x represents the top of the atmosphere) and by θ the zenith angle of the emitted radiation the solution is (dropping the spectral index):

$$L(z_x, \theta) = L(0, \theta)\tau(0, z_x, \theta) + \int_0^{z_x} \frac{k\rho}{\cos\theta} B(T_z)\tau(z, z_x, \theta)\ \mathrm{d}z$$

$$\tau(a, b, \theta) = \exp\left(-\int_a^b \frac{k\rho}{\cos\theta}\ \mathrm{d}z\right)$$

The term $\mathrm{d}z/\cos\theta$ is the increase of optical depth with zenith angle for a plane parallel atmosphere.

One may note that

$$W_\nu(z, z_x, \theta) \equiv \frac{\mathrm{d}\tau_\nu(z, z_x, \theta)}{\mathrm{d}z} = \frac{k_\nu\rho}{\cos\theta}\tau(z, z_x, \theta)$$

and that the contribution from the lower radiating surface (either land or sea) can be expressed as $L_\nu(0) = \varepsilon_{s,\nu}B_\nu(T_0)$ where $\varepsilon_{s,\nu}$ is its emissivity; so that finally

$$L_\nu(z_x, \theta) = \varepsilon_{s,\nu}B_\nu(T_0)\tau(0, z_x, \theta) + \int_0^{z_x} B_\nu(T_z)W_\nu(z, z_x, \theta)\ \mathrm{d}z \tag{10}$$

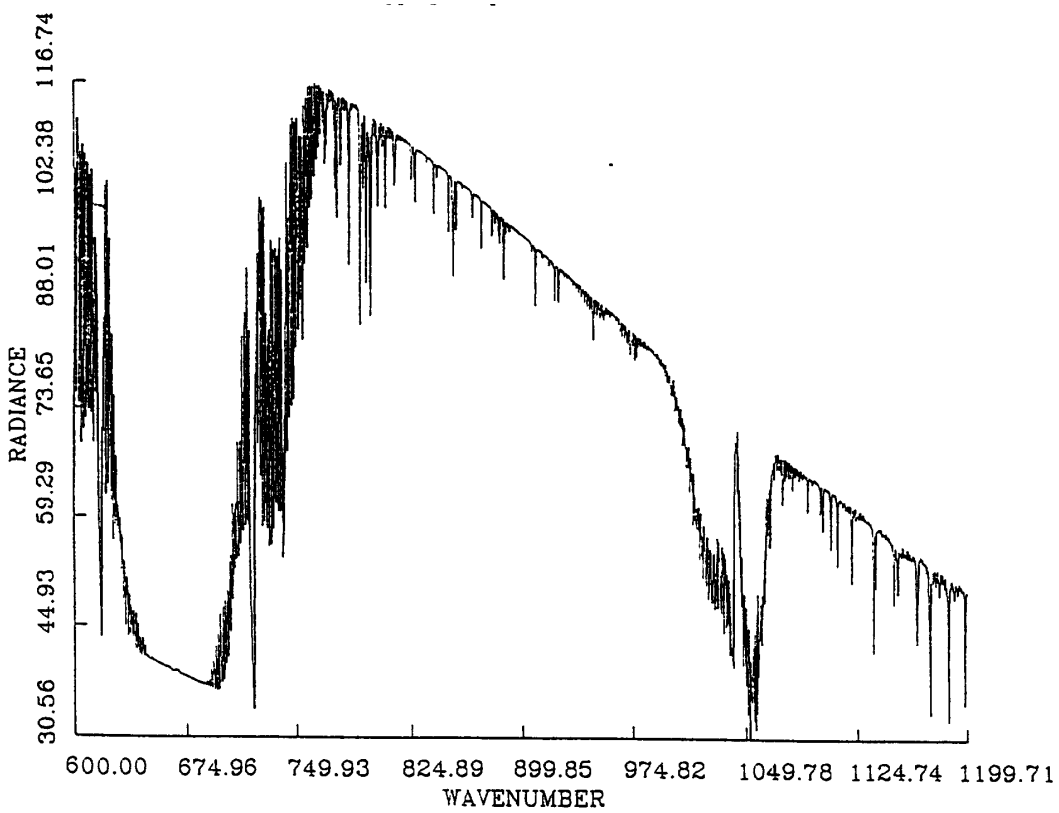

Figure 5. The simulated upward radiance at 56 hPa height for a mid-latitude temperature and moisture profile.

The contribution of each layer dz of the atmosphere, centred at z, to the integrated upward radiance emerging to space, is hence expressed by a blackbody contribution weighted according to W; layers for which W attains largest

values are the ones who contribute most to the integral value at the top. W is often called the weighting function. Equation (10) can also be expressed using pressure, or $\log p$, as vertical coordinate. Examples can be found in Section 10.

6. Spectral distribution of radiance leaving the atmosphere

Radiance, defined in Section 2, can be expressed in terms of the temperature that a perfect black body would have to emit the same radiance in the same wavenumber interval. The latter quantity is referred to as brightness temperature ($T_B(K)$).

Figure 5 shows simulated upward radiance at 56 hPa height for a mid-latitude temperature and moisture profile. Fig. 6 shows the same data converted to T_B. The spectral resolution (see section 10 for the definition) of the two data set is ≈ 0.67 cm^{-1}.It may be noticed that a constant T_B corresponds to diminishing values of radiance as we move to higher wavenumbers since the maximum value for the Planck function at 300 K is around 600 cm^{-1}.

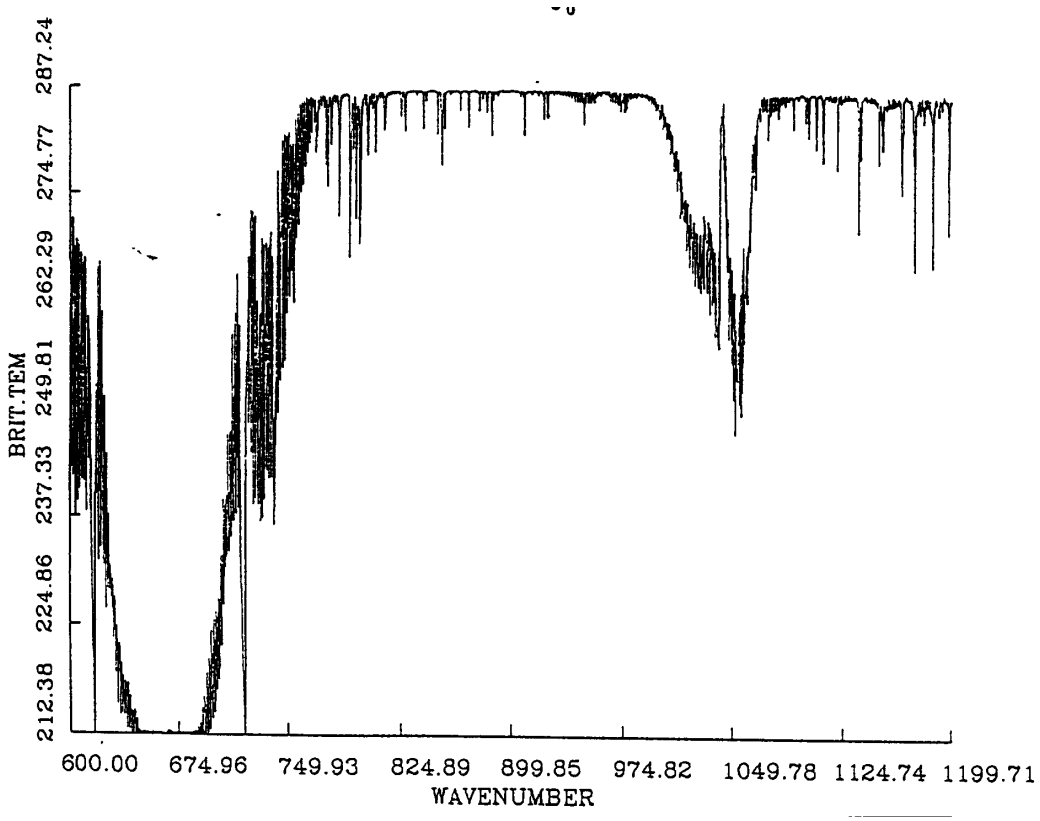

Figure 6. The data in Fig. 5 converted to T_B.

The spectral range shown in the two figures covers an important domain used for atmospheric sounding purposes, namely the whole CO_2 absorption band centred at 672 cm^{-1} (15 μm) and the window region from 1050 to 770 cm^{-1} (about 9.5 to 13 μm). Another important feature is the ozone absorption band around 1040 cm^{-1} (9.6 μm). Figure 7 shows two emission spectra of the earth and atmosphere as measured from the IRIS interferometer on board NIMBUS 3 (taken from Hanel, 1971). The upper figure is radiance measured over Antarctica while the lower one is measured over the Sahara desert.

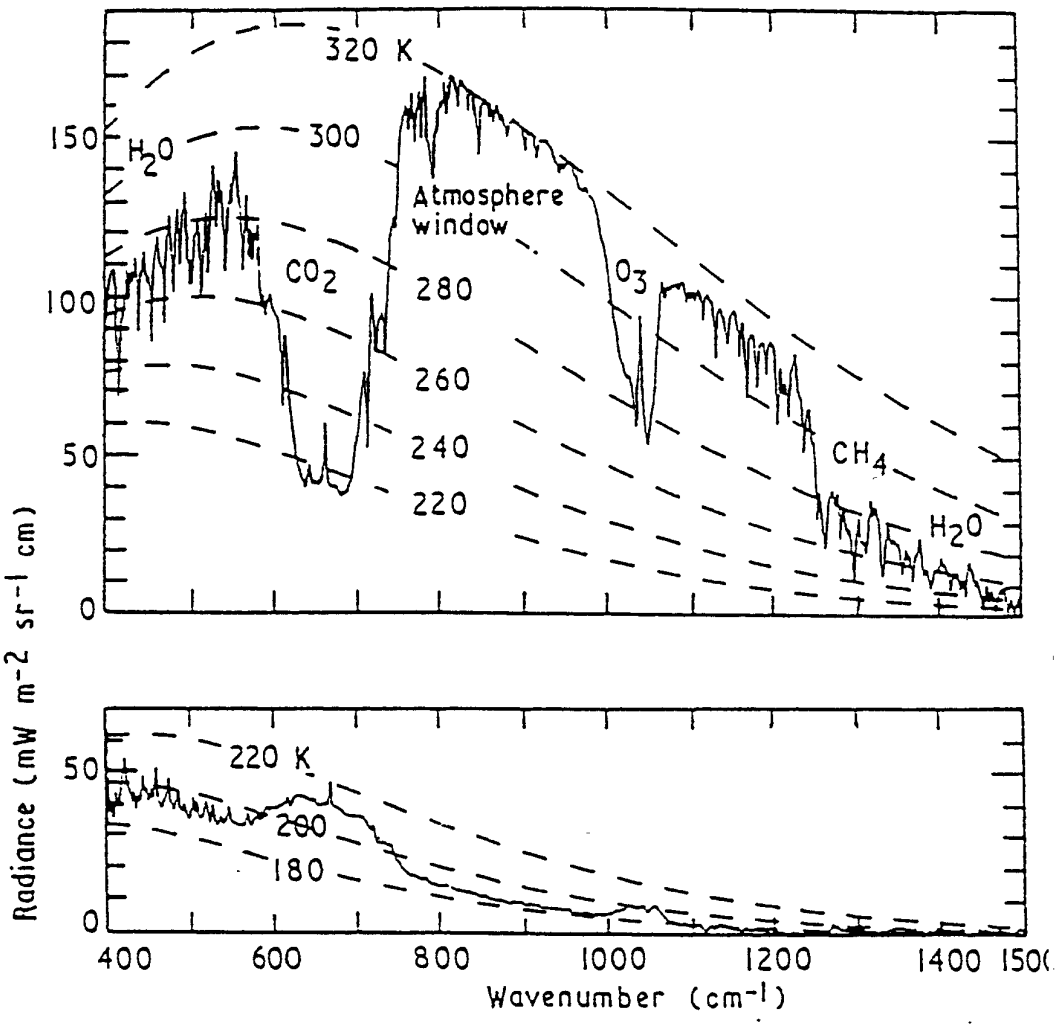

Figure 7. Two emission spectra of the earth and atmosphere as measured from the IRIS interferometer on board NIM

Recalling that low values of T_B are associated with low numeric values of radiances, it appears that some complex interaction is taking place within the atmosphere producing large variations in energy emitted upwards. An explanation for this requires some knowledge of basic spectroscopy, the principles of which will be dealt with in the next section. It will be shown that the presence of sharp variations in brightness temperature (or radiance, or absorption properties) is due to the nature of the interaction which is quantized.

7. MODELLING THE INTERACTION

For interaction to take place a force must act on a molecule in the presence of an external electromagnetic field. The existence of such a force depends on the presence of an electric or magnetic instantaneous dipole moment. The polarizability of a molecule is related to the extent to which a molecule has a permanent dipole moment or can acquire an oscillating one produced by its vibrational motion. If we consider a molecule as a rigid rotator, radiative interaction can take place only if the molecules possess a permanent dipole moment. Thus CO, N_2O, H_2O and O_3 (see Fig. 8) interact with the field by changing their "rotation vector" while N_2, O_2, CO_2 and CH_4 do not. However

as a molecule like CO_2 vibrates, an oscillating electrical dipole moment is produced and rotational interaction can take place. Hence CO_2 and CH_4 possess vibration-rotational couplings with the incident wave.

In what follows only interaction through electric dipole moments will be considered, the main aim of this section being to show some examples of how molecular absorption and emission spectra can be explained (and computed).

7.1 The molecule as a rigid quantized rotator.

Diatomic or linear triatomic molecule (Fig. 10) have two equal moments of inertia and two degrees of rotational freedom. Asymmetric top molecules, like H_2O have three unequal moments of inertia and three degrees of freedom.

The kinetic energy E_{rot} of a rigid rotator is $E_{\text{rot}} = \frac{1}{2} I \omega^2$. While for a classical rotator ω and hence E_{rot} can take any value, a quantized rotator is subject to quantum restrictions on angular momentum

$$I\omega = \frac{h}{2\pi}[J(J+1)]^{1/2}$$

where J, the quantum number for rotation, can assume only integer values. The quantized rotational energy can therefore be written

$$E_J = E_{\text{rot},J} = \frac{1}{2}\frac{(I\omega)^2}{I} = \frac{h^2}{8\pi^2 I} J(J+1)$$

Recalling that E_J is the rotational energy associated to a rotational state J around a specific principal axis and calling rotational constant the quantity

$$A = \frac{h}{8\pi^2 c I_{\text{A}}}$$

where I_A is the moment of inertia around that axis, we may write

$$E_J = AhcJ(J+1)$$

For asymmetric top molecules we will have three moments of inertia (I_A, I_B, I_C) and three rotational constants (namely A , B and C). The rotational energy can be expressed in terms of the rotational term $F(J)$

$$F(J) = \frac{E_J}{hc} = BJ(J+1)$$

which is measured in the energy unit cm^{-1}. B is the rotational constant associated to the axis with moment of inertia I_B . In Table 1 values of the molecular electrical dipole and rotational constants for some of the most important active atmospheric species are given.

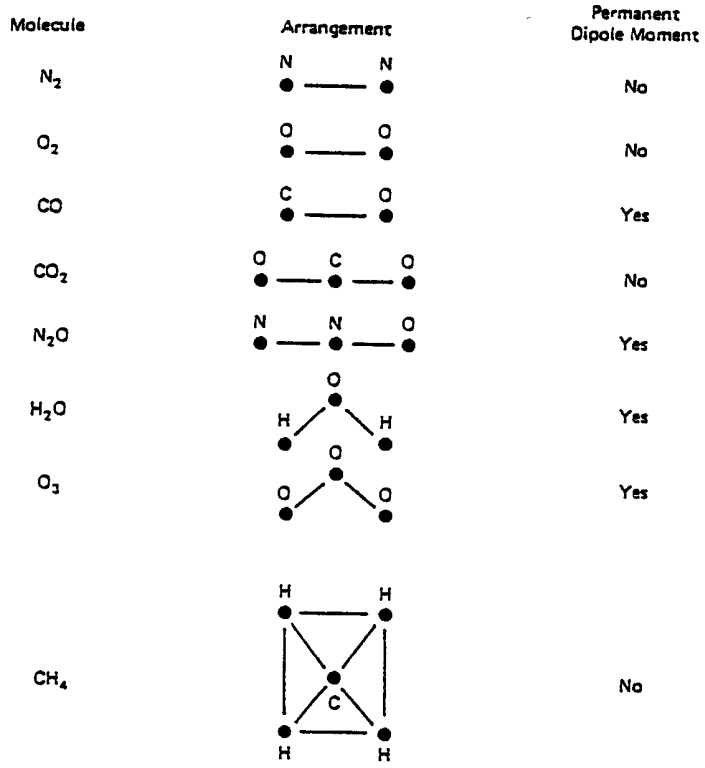

Figure 8. Symbolic nuclear configurations and permanent dipole moment status of some atmospheric molecules (figure taken from McCartney, 1983).

TABLE 1. VALUES OF MOLECULAR ELECTRICAL DIPOLE MOMENT (M IN DEBYE UNITS) AND ROTATIONAL CONSTANTS OF SOME ATMOSPHERIC MOLECULES

Species	μ	A	B	C
CO	0.112	–	1.9314	–
CO_2	0.	–	0.3902	–
N_2O	0.167	–	0.4190	–
H_2O	1.85	27.877	14.512	9.285
O_3	0.53	3.553	0.445	0.395
CH_4	0.	–	5.249	–

Interaction between the molecule and the external field takes place whenever a quantum of energy $h\nu c$ is extracted (absorption process) or added (emission) to the external field. The basic relation holds

$$E' - E'' = h\nu c$$

where E' and E'' are the two energy levels involved. Denoting the upper and lower rotational quantum number as J' and J'' the difference between the two energy levels is

$$\Delta F = BJ'(J'+1) - BJ''(J''+1)$$

A quantum selection rule dictates that only transition among adjacent levels are allowed, that is

$$\Delta J = (J' - J'') = \pm 1$$

where the value $\Delta J = +1$ applies to absorption, which increases the internal energy of the molecule. Hence for the case of absorption

$$\Delta F = 2B(J'' + 1) = 2BJ' = \nu_{rot} \tag{11}$$

The absorbed photons have energies that are individually equal to Eq. (11) and the aggregate effect from all the molecules in a volume is a depletion of the incident wave energy at wavenumber ν_{rot} which is observed as a spectral line. As an example absorption of a photon at wavenumber 669.29 (corresponding to the wavelength 14.947 μm) is accomplished by the H_2O molecule spinning around its principal axis *A* with a transition from rotational quantum number 12 to 13.

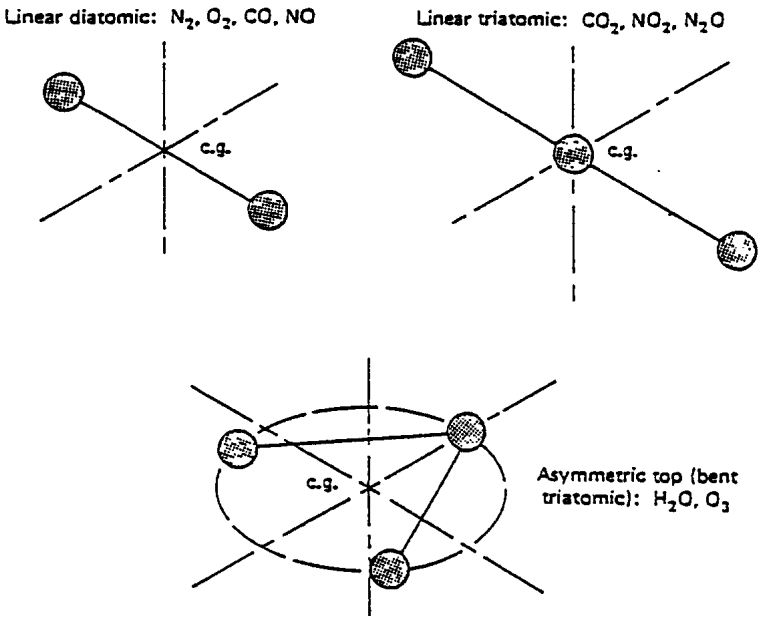

Figure 9. Axes of rotational freedom for linear and asymmetric top molecules (figure taken from McCartney,1983).

7.2 The molecule as a quantized vibrator.

An ensemble of nuclear masses held together by elastic valence bonds forms a system capable of vibrating in one or more modes. Some of the most commonly encountered vibrational modes for diatomic and triatomic molecules are shown in Fig. 10 .

A classical two-mass vibrator has a natural frequency $\tilde{\nu}$ which is given by:

$$\tilde{\nu} = \frac{1}{2\pi}\left(\frac{k_e}{m'}\right)^{\frac{1}{2}}$$

where k_e is the elastic force constant and m' is the reduced mass. The potential energy for this system is given by

the relation

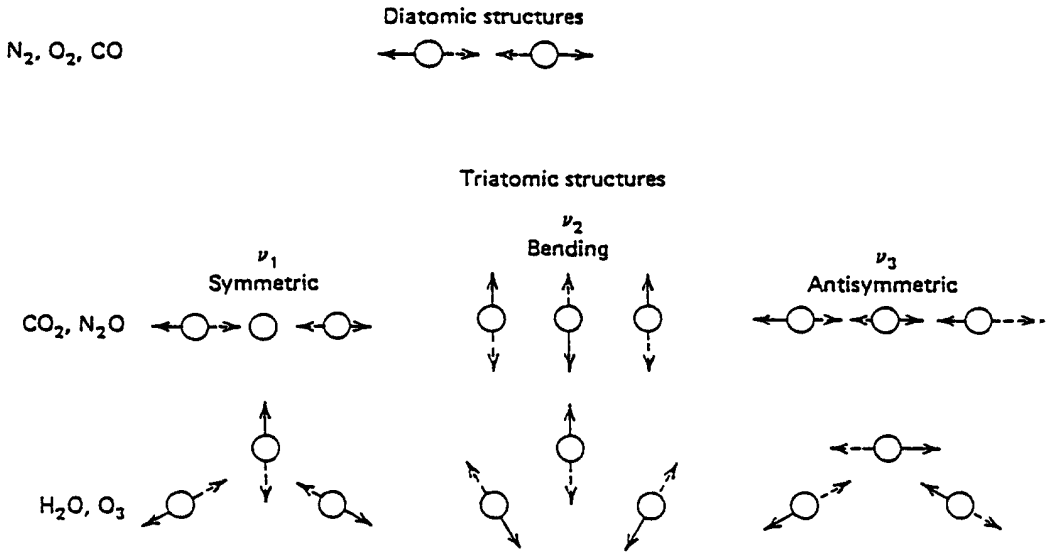

Figure 10. Symbolic configurations and vibrational modes of diatomic and triatomic molecules (figure taken from McCartney, 1983).

$$E_p = 2\pi^2 m'(r - r_0)^2 \tilde{\nu}^2$$

where r_0 is the distance between the two masses at equilibrium. Quantum restrictions on vibrational energy are found by solving the time independent Schroedinger equation in one dimension. The eigenvalues defining the allowed energy levels are

$$E_\nu = \left(\nu + \frac{1}{2}\right) h\tilde{\nu} \qquad \nu = 0, 1, 2, \ldots$$

$$E_\nu = \left(\nu + \frac{1}{2}\right) \frac{h}{2\pi} \left(\frac{k_e}{m'}\right)^{\frac{1}{2}}$$

where ν is the quantum number for vibration. These equations hold for a simple harmonic motion, which is true only when the vibrational quantum number is small. Disregarding some of the complexities of real life, we may consider a simple transition of a diatomic molecule from two adjacent vibrational levels since the quantum selection rule allows only transition for which $\Delta\nu = \pm 1$, where the plus sign applies for transition in which the internal energy is incremented through absorption of a quantum of energy. Denoting by ν' any level except $\nu = 0$ and by ν'' the next lower level, the transition energy is

$$\Delta E = \frac{h}{2\pi} \left(\frac{k_e}{m'}\right)^{\frac{1}{2}} \left[\left(\nu' + \frac{1}{2}\right) - \left(\nu'' + \frac{1}{2}\right)\right]$$

.

TABLE 2. VIBRATIONAL FREQUENCIES, WAVELENGTHS AND WAVENUMBERS OF RADIATIVELY ACTIVE ATMOSPHERIC MOLECULES (TAKEN FROM McCartney, 1983).

Species	Parameter	Vibrational modes		
		ν_1	ν_2	ν_3
CO	Hz	6.43×10^{13}	-	-
	μm	4.67	-	-
	cm^{-1}	2143	-	-
CO_2	Hz	-	2.00×10^{13}	7.05×10^{13}
	μm	-	15.0	4.26
	cm^{-1}	-	667	2349
N_2O	Hz	3.86×10^{13}	1.77×10^{13}	6.67×10^{13}
	μm	7.78	17.0	4.49
	cm^{-1}	1285	589	2224
H_2O	Hz	1.10×10^{14}	4.79×10^{13}	1.13×10^{14}
	μm	2.73	6.27	2.65
	cm^{-1}	3657	1595	3776
O_3	Hz	3.33×10^{13}	2.12×10^{13}	3.13×10^{13}
	μm	9.01	14.2	9.59
	cm^{-1}	1110	705	1043
NO	Hz	5.71×10^{13}	-	-
	μm	5.25	-	-
	cm^{-1}	1904	-	-
NO_2	Hz	3.92×10^{13}	2.26×10^{13}	4.86×10^{13}
	μm	7.66	13.25	6.17
	cm^{-1}	1306	755	1621
CH_4	Hz	8.75×10^{13}	4.60×10^{13}	9.06×10^{13}
	μm	3.43	6.52	3.31
	cm^{-1}	2917	1534	3019
		ν_4		
CH_4	Hz	5.71×10^{13}		
	μm	5.25		
	cm^{-1}	1904		

hence

$$\Delta E = \frac{h}{2\pi}\left(\frac{k_e}{m'}\right)^{\frac{1}{2}}$$

Therefore a photon of energy $h\nu_{vib}c$, where ν_{vib} denotes the wavenumber of the transition, will be absorbed if

$$\Delta E = h\tilde{\nu} = h\nu_{vib}c$$

that is when

$$\nu_{vib} = \frac{1}{2\pi c}\left(\frac{k_e}{m'}\right)^{\frac{1}{2}}$$

The absorption by a volume of gas will result in the depletion of radiation of wavenumber ν_{vib} (or frequency $\tilde{\nu}$) which appears as an absorption line in the spectrum. As an example let's consider the CO molecule. Its reduced mass is $m' = 1.14 \times 10^{-23}$ grams and the force constant has a value of $k_e = 1.84 \times 10^6$ dyn cm^{-1}. Substituting these values in the last equation we obtain for a transition from level $\nu = 0$ to $\nu = 1$ an energy increase $\Delta E = 4.24 \times 10^{-23}$ ergs equivalent to $\nu_{vib} = 2143$ cm^{-1}. In Table 2 the vibrational frequencies, wavelengths and wavenumbers of interesting atmospheric radiative molecules are listed.

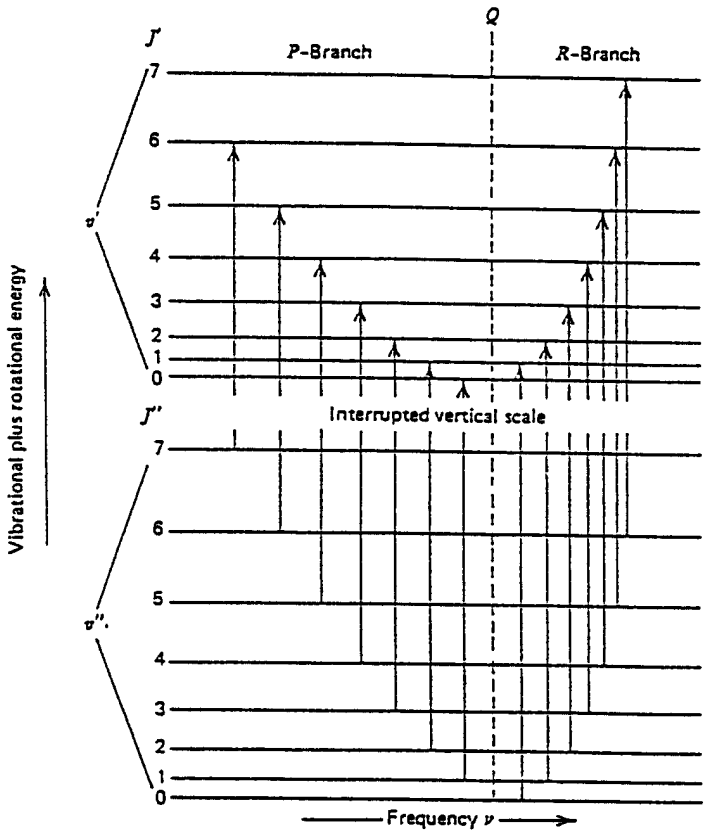

Figure 11. Simultaneous transitions in vibrational and rotational energies (figure taken from McCartney, 1983).

7.3 Vibro-rotational bands.

It has been already pointed out that molecules not possessing a permanent dipole moment do in fact possess oscillating dipole moments, caused by their vibrational motion, and therefore rotational transition coupled to vibrational transition are possible. Considering a simple molecule with one degree of rotational freedom (CO_2 for example) we may therefore observe absorption (and emission) corresponding to quantum energies

$$\Delta E = h\nu c = \Delta E_{vib} + \Delta E_{rot}$$

where the terms on the right side are taken with their sign. That is a number of transitions are allowed depending

on the number of degrees of rotational freedom and on the number of vibrational modes. A simple description of the allowed energy transitions are shown in Fig. 11 .

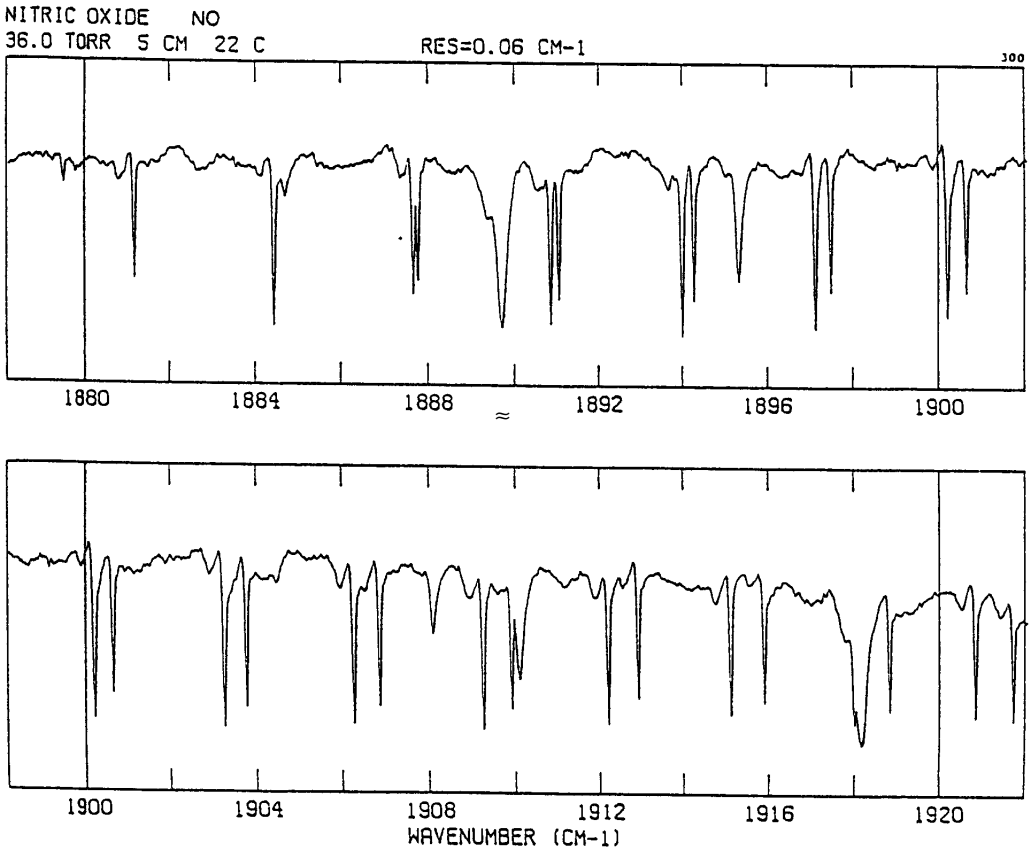

Figure 12. Nitric oxide spectrum.

The more complex the molecular structure the larger the number of possible transitions. As an example Fig. 12 shows the superposition of NO rotational lines close to the vibrational wavenumber at ≈ 1904 cm^{-1} with a resolution of 0.06 cm^{-1} while in Fig. 13 the complex structure due to the three rotational modes of NO_2 is superimposed to its vibrational transition at ≈ 1621 cm^{-1}. In the latter the resolution of the measurements is 0.02 cm^{-1}.

Water vapour is one of the most important radiatively active molecules. Its complicated rotational (three degrees of freedom) and vibrational (three modes) structure produce a line spectrum which, at first sight, appears randomly distributed. One of the most important H_2O absorption feature is the vibro-rotational band at ≈ 1595 cm^{-1}. The central portion of the complex band, close to the vibrational frequency, is shown in Fig. 14 at a resolution of 0.46 cm^{-1}.

At longer wavelengths, micro- and millimetre-wave frequencies, single rotational lines are also observed. Three of these, due to H_2O and O_2, are going to play an increasingly important role in microwave remote sensing, namely the line centred at 64 and 112 (O_2) and 183 (H_2O) GHz which are shown in Fig. 15 .

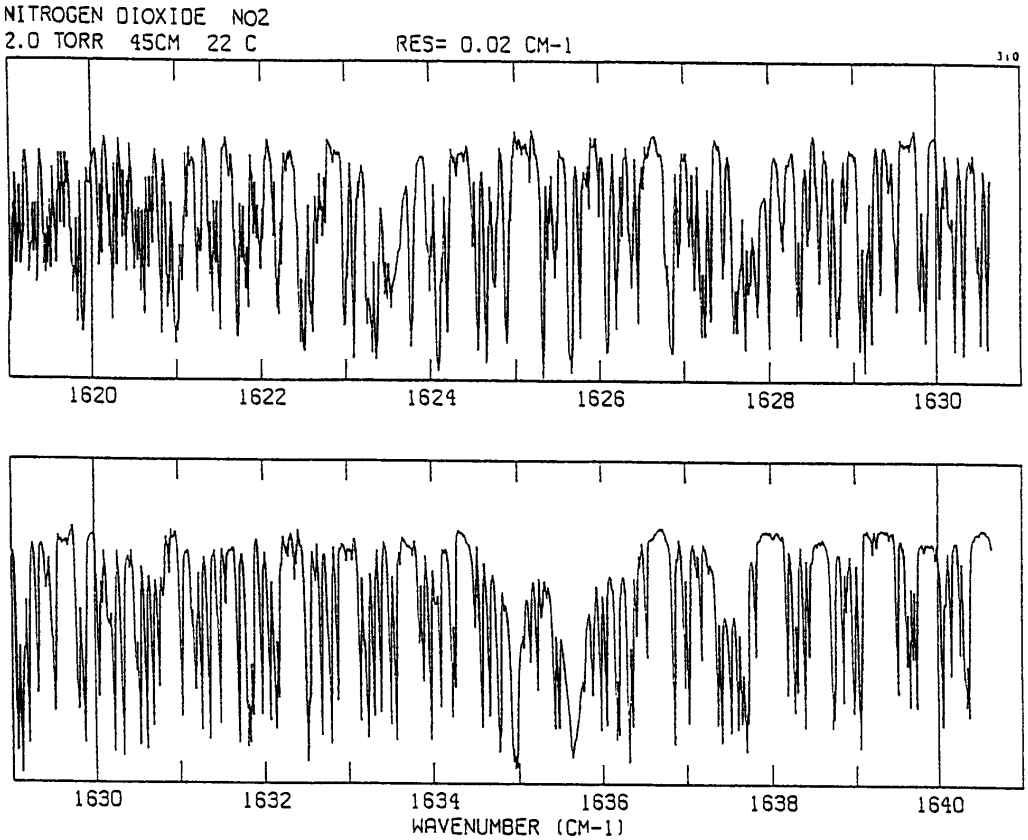

Figure 13. Nitrogen dioxide spectrum.

8. LINE SHAPES AND THE ABSORPTION COEFFICIENT.

For a strictly monochromatic absorption and emission to occur at ν_0, the energy involved for each molecule of gas should be exactly $\Delta E = E' - E'' = h\nu c$, implying that the energy levels are exactly known. The mathematical description of the absorption line would be $k\nu = S\delta(\nu - \nu_0)$ where S is the line strength and δ is the Dirac delta function centred at ν_0. However three physical phenomena occur in the atmosphere (and elsewhere) which produce broadening of the line: (i) natural broadening, (ii) collision broadening and (iii) doppler broadening, which will be briefly discussed.

8.1 Natural broadening.

It is caused by smearing of the energy levels involved in the transition. In quantum mechanical terms this is due to the uncertainty principle and depends on the finite duration of each transition. It can be shown that the appropriate line shape to describe natural broadening is the Lorentz line shape

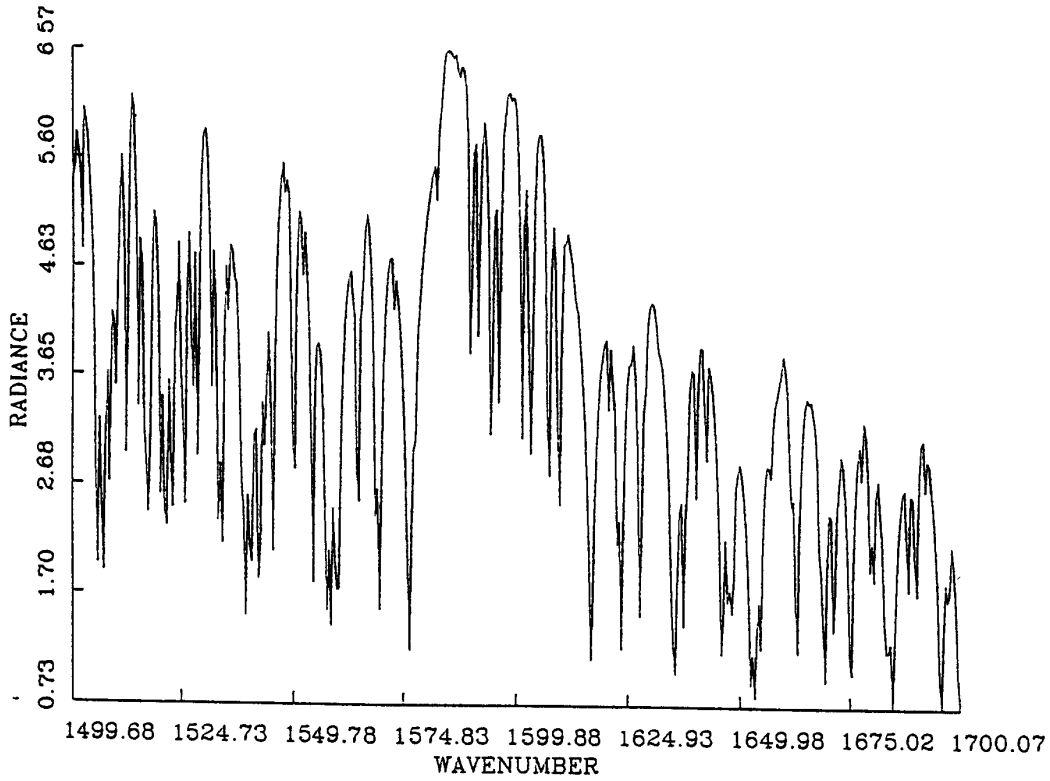

Figure 14. Emission spectrum of the atmosphere measured at 10 km height with a resolution of approximately half wavenumber. Most of the lines are due to the water vapour vibro-rotational band.

$$k_\nu \equiv k(\nu) = \frac{S}{\pi} \times \frac{\alpha_n}{(\nu - \nu_0)^2 + \alpha_n{}^2}$$

where S is the line strength

$$S = \int_{-\infty}^{\infty} k(\nu)\, d\nu$$

and α_n is the line half width, which is the distance from the line centre λ_0 to λ_h where $k(\nu)$ has decreased to half of its maximum power. The shape of a Lorentzian line is shown in Fig. 16 . It can be shown that α_n is independent of wave number and its value is of the order of 10^{-5} nm

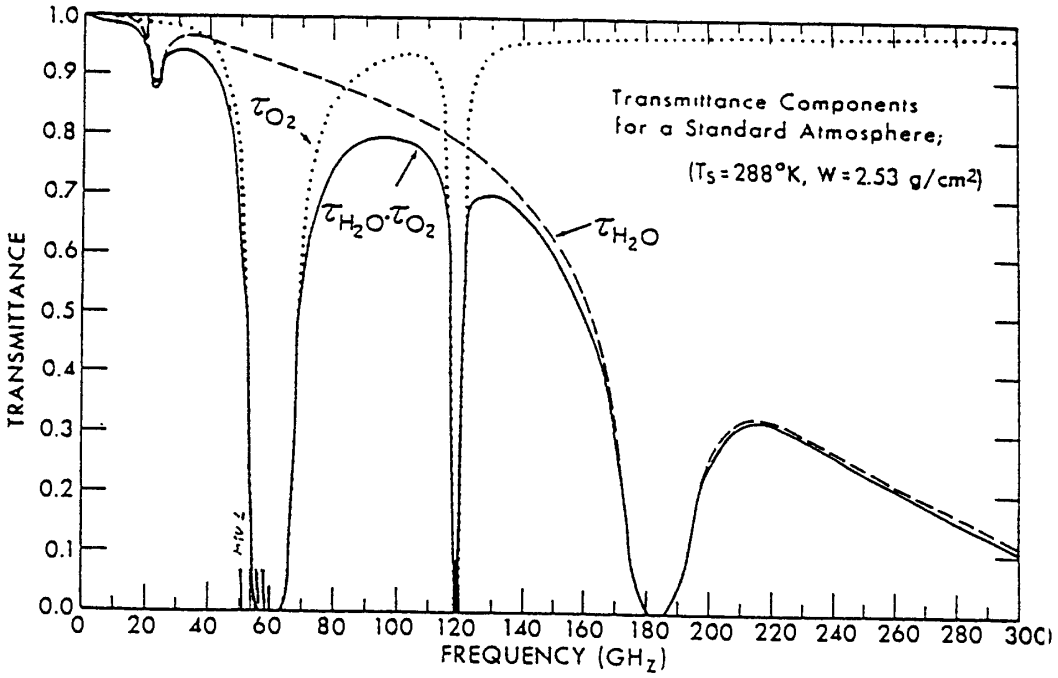

Figure 15.Transmittances of the millimetre wave region calculated for a path between the surface and space for molecular oxygen, water vapour and their product (taken from Grody, 1976).

8.2 Collisional broadening.

It is due to the modification of molecular potentials, and hence to the energy levels, which take place during each emission (absorption) process, and is caused by inelastic as well as elastic collisions between the molecule and the surrounding ones. The shape of the line is still Lorentzian, as for natural broadening, but the half width α_c is several orders of magnitude greater, and is inversely proportional to the mean free path between collisions, which indicates

that α_c will vary depending on pressure p and temperature T of the gas. When the partial pressure of the absorbing gas is a small fraction of the total gas pressure we can write:

$$\alpha_c = \alpha_{c,s} \frac{p}{p_s} \sqrt{\frac{T_s}{T}}$$

where p_s and T_s are reference values. As an example the collisional half width for the CO molecule in the vicinity of the vibrational ν_1 vibrational transition, at standard pressure and $T = 300$ K is $\alpha_c \approx 4.22 \times 10^{-2}$ nm

8.3 Doppler broadening.

Molecules in a volume of air possess a Maxwell velocity distribution, hence the velocity components along any direction of observation produce a Doppler effect which induces a shift in frequency in the emitted and absorbed radiance. The line shape is

$$k(\nu) = \frac{S}{\alpha_d \sqrt{\pi}} \exp\left[\frac{-(\nu - \nu_0)^2}{\alpha_d{}^2}\right]$$

$$\alpha_d = 3.58 \times 10^{-7} \nu_0 (T / M_A)^{\frac{1}{2}}$$

where M_A is the molar mass. The Doppler half width for the CO transition of the previous paragraph is $\alpha_d \approx 5.5 \times 10^{-3}$ nm which is about 1/8 of the collisional half width. Collisions are the major cause of broadening in the troposphere, since their effect is proportional to pressure, and pressure variations are larger than temperature variations; while Doppler broadening is the dominant effect in the stratosphere, due to the larger mean free path and high temperatures, the latter producing larger standard deviations for the molecular velocity distribution. There is however an intermediate region where neither of the two shapes is satisfactory since both processes are active at once. Assuming the collisional and doppler broadening can be assumed to be independent we can combine both line shapes to give the Voigt shape. This is often used to allow for both tropospheric and stratospheric broadening of an absorption/emission line in one calculation.

Actually the level of our knowledge of spectroscopic phenomena, that are at the very core of our understanding of the radiative processes, is still insufficient for many purposes, and a large effort is taking place to perform more accurate measurements of the key parameters, in order to avoid, whenever possible, the use of empirical tuning to reduce discrepancies between measurements and model results.

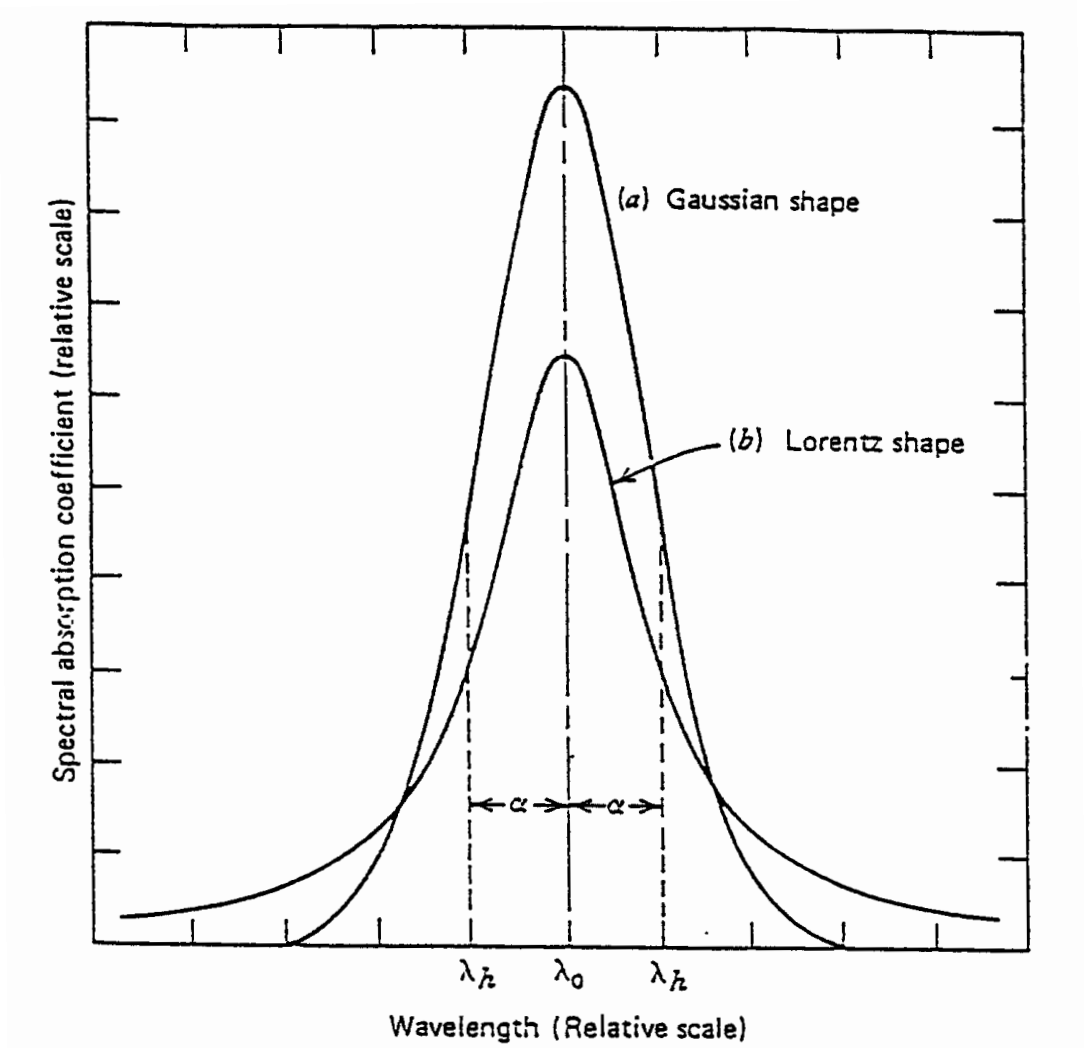

Figure 16. Spectral line shape produced by: (a) Doppler broadening and (b) natural and collision broadening (taken from Levi (1968).

9. CONTINUUM ABSORPTION

In addition to discrete molecular interactions with radiation there is also another important, but less understood, mechanism for interacting with the incident radiation field called continuum absorption/emission by some atmospheric molecules, most notably water vapour. Continuum absorption manifests itself in the infrared and millimetre wave window regions of the atmospheric spectrum causing the windows to be less transparent than predicted by discrete molecular absorption alone. For channels designed to sense the surface this is obviously an important factor. This continuum absorption/emission has a smooth frequency dependence making it impossible to ascribe to specific molecular transitions.

There are two main theories for continuum absorption/emission. One is that it is due to the residual effects of the far wings of strong lines which are not accurately modelled. If there are many strong lines some distance away (in frequency) the effect of the individual lines can accumulate. A second theory is that the interaction is caused by molecular polymers (e.g. water vapour dimer) which being large floppy molecules might be expected to have broad

transitions and hence broad spectral features. The exact mechanism continues to be a matter of debate.

Laboratory and field measurements have measured the excess absorption and empirical relationships have been developed to provide an estimate of the continuum absorption for any atmospheric path. One problem is that most of the measurements are for warm paths (300 K) whereas most atmospheric paths are colder than this. Nevertheless empirical relationships are widely used to include this source of absorption/emission in the estimation of the atmospheric transmittance. The gases which have significant continuum absorption are H_2O, CO_2, N_2, and O_2 and the continuum is included for all window channel transmittance calculations from the visible to microwaves.

As an example, for the Advanced Very High Resolution Radiometer (AVHRR) infrared window channel at 925 cm^{-1}, the mean transmittance due to molecular line effects is 0.97 whereas the transmittance due to the continuum is only 0.93 for a mid-latitude atmosphere.

10. INTEGRATION OVER FREQUENCY

A common requirement for radiometers that are used for sounding the atmosphere is the high radiometric performance, which can be expressed as a required noise performance or, equivalently, in terms of signal–to–noise ratio. The latter concept is useful in clarifying that, in order to reach a given performance, it may be necessary to integrate the signal in the wavenumber domain, and/or in time; another way is to allow more energy to reach the detector by increasing the solid angle of the measurement. The instruments used to sense operationally the atmosphere are usually subdivided into two categories: sounders, where the frequency integration is kept to a minimum for reasons that will be discussed in Section 11, and imagers where the solid angle is minimized. In both cases some degree of integration in the wave-number domain is required. To simulate the behaviour of the radiometer, and to extract successfully information from the set of radiance measurements, it is therefore necessary to compute integrated quantities, like radiance in the interval $\Delta\nu$

$$L_{\Delta\nu} \equiv \frac{\int_{\Delta\nu} R_\nu L_\nu d\nu}{\int_{\Delta\nu} R_\nu d\nu}$$

where R_ν is the transmission of the filter for the radiometer channel. There are several ways in which the integration can be performed, of different attainable accuracy, and will be only briefly outlined. Although much confusion is associated to the concept of resolution, the term has been used throughout in these notes to indicate a spectral width over which either an instrument averages the natural signal, or higher resolution computations have been averaged. Two examples of frequency integration are shown in Fig. 17 .

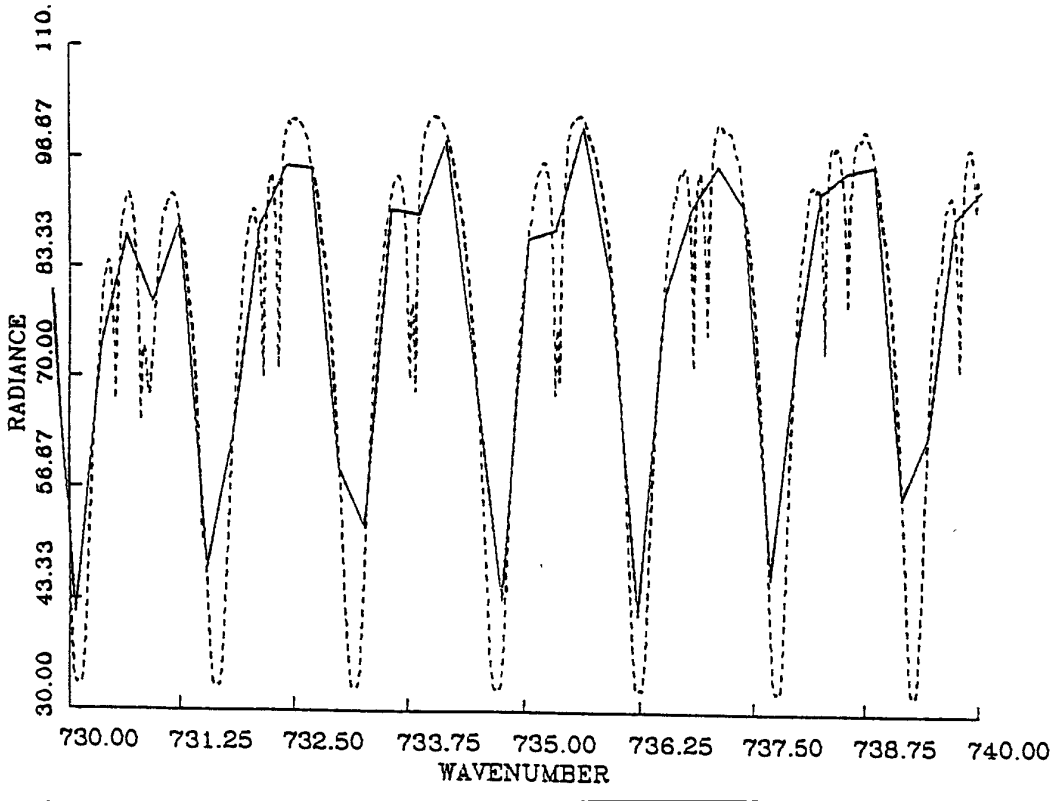

Figure 17. Examples of frequency integration: the broken curve is radiance computed at a resolution of 0.005 cm^{-1}, while the resolution of the full line is 0.293 cm^{-1}. Both refer to the same measuring geometry and atmospheric conditions as Fig. 5

10.1 Line-by-line methods

A line-by-line model computes the contribution of each absorption line, within a predefined interval, to the monochromatic optical depth σ_ν, at a given wave number ν. The total number, and the wave-number location, of the monochromatic computations depends on the accuracy to be obtained in the final product, the mean optical depth, or transmittance, in a wave-number interval that can be as small as required to accurately simulate the radiometer frequency response. It is the only way to proceed when the aim is accuracy and computer time is less of a problem. It exploits the information content of the spectroscopic databases (GEISA 1984; HITRAN 1986) and allows the deficiencies of the spectral parameters to be analysed, provided good laboratory or field data is available.

10.2 Fast-transmittance models.

A line-by-line model can also be used to compute accurate transmittances for a moderate number of atmospheric temperature and humidity profiles, chosen to represent widely differing atmospheric situations, and then derive coefficients for parametric formulas relating the computed transmittances to the input data; the same parametrization is then used for any atmospheric situation. The line-by-line computations must produce transmittances integrated over wavenumber intervals much smaller than the channel width of the radiometer to be modelled so that the correct instrument function can be applied when computing the averaged transmittances for any channel. The final result of an integration over wavenumber, either performed by the instrument itself or done on computed data, is a set of average transmittances, or radiances, for each channel of the instrument. The fast model transmittances can

be used in Eq. (12) to compute an upwelling radiance for the radiometer channel.

11. THE DIRECT PROBLEM.

We have seen that for a cloudless atmosphere the equation for upwelling radiance at the upper boundary of the atmosphere can be written in the form

$$L_\nu(\theta) = \varepsilon_{s,\nu} B_\nu(T_s)\tau_\nu(p_s,\theta) + \int_{p_s}^{0} B_\nu(T_p)\frac{\partial \tau_\nu(p,\theta)}{\partial \ln p}\, d\ln p \qquad (12)$$

$$\tau_\nu(p,\theta) = \exp\left(-\int_0^p k_\nu \frac{q}{g}\sec\theta\, dp\right)$$

where $q(p)$ is the vertical profile of mass mixing ratio of the absorbing (emitting) material (water vapour, CO_2, N_2O, O_3, etc.), and the subscript s indicates the lower boundary of the atmosphere. Eq. (12) clearly indicates that the interpretation of the radiance emitted by the atmosphere at a given wavenumber requires a detailed knowledge of:

(a) spectroscopic properties of all gases radiatively active (which is contained in the term $\tau_\nu(p,\theta)$, and the transmittance is also function of temperature and absorbing constituent amount along the ray path;

(b) the vertical profile of the concentration for each radiatively active gas (term $q(p)$),

(c) the temperature structure $T(p)$ up to a level where emission phenomena become negligible.

(d) the lower surface radiative properties, that is emissivity and skin temperature.

We will now assume that it is possible to derive an equation similar to (12) when dealing with integrated radiance over a small wave-number interval, and will now try to understand the features of the radiance or brightness temperature spectra shown previously.

There are tens of gaseous species which are radiatively active in this region of the spectrum, although the main absorbers are CO_2, CH_4, N_2O, O_3 and H_2O. The first three can be considered as uniformly distributed along the vertical. With reference to Fig. 5 (or 6) the temperature structure can be approximated by the standard atmosphere with the vertical lapse rate of ≈ -8 K/km. Highest values of B_T are observed in the range 800–1000 and

1080–1120 cm^{-1}, the so-called infrared window region, since we know, from our spectroscopic knowledge, that only relatively weak lines are present in that range; consequently most of the emission by the lower (warm) surface reaches the top of the atmosphere. Skin temperature can be derived from the hottest points in the curve (assuming that surface emissivity is close to unity) giving a value of ≈ 283 K. Lowest B_T values are measured in the strongest absorption region of carbon dioxide, from 660–680 cm^{-1} since, at these wave numbers, radiation emitted by atmospheric layers close to the ground (and relatively warm) is completely absorbed on its way to mid-troposphere by the strong and thick lines, and only radiation emitted in the upper tropospheric layers, which are relatively cold, reaches space (in the upper layers lines are thinner); therefore the measured brightness temperature is low.

There are an infinite number of intermediate cases in which the weighting function peaks somewhere in mid-troposphere, since lines are strong and broad enough to absorb all the surface emission, but radiance originating from mid tropospheric layers is only partially absorbed, by the now thinner lines, on its way to space. And so on.

The top panel of Fig. 7 needs some further explanation, but along the same lines. When the measurements were made, over Antarctica, the temperature of the surface was lower that the air temperature in the stratosphere, which

means that the radiance signal coming from the most absorbing regions is actually warmer than the window values.

From this brief discussion it appears therefore that a series of measurements of the emitted upwelling radiance, distributed from the centre to the wings of an absorption band, contains intermixed information on the vertical temperature and concentration structure. In any case the relation between radiance, temperature and concentration is highly nonlinear as shown formally by Eq. (12).

The worst limitation to the use of Eq. (12) is due to the fact that even shallow clouds are opaque to infrared radiation. With the exception of thin cirrus, clouds act as a blackbody effectively masking all radiative information coming from below cloud top. Since the typical horizontal dimension for an infrared sounder field of view ranges from several km to several tens of km, to collect enough energy to maintain a sufficiently high signal–to–noise ratio, a completely clear atmosphere over the field of view of a sounding instrument is a rarity, especially in meteorologically active areas where temperature profiles are most needed for accurate weather forecasting. In the microwave, although scattering by non-precipitating clouds is almost negligible, scattering due to precipitation makes a noticeable contribution to microwave radiance, hence calculation of temperature without accounting for the scattering results in large errors. These effects are enhanced when millimetre–wave radiometers, as the 183 GHz radiometer, which can be used to derive water vapour profile, are used to sound the atmosphere. Uncertainties caused by the undetected presence of clouds are the greatest source of error in remote sensing of the lower and middle troposphere. Nevertheless the new millimetre wave radiometers which are starting to fly offer great potential for global NWP applications as the areas where cloud effects can be neglected will be much greater than for the infrared instruments allowing better global coverage.

REFERENCES

Goody R.M. and Yung Y.L. 1989 *Atmospheric radiation theoretical basis*. Second edition. Oxford University Press

Grody, N.C., 1976, Remote sensing of atmospheric water content from satellites using microwave radiometer. *IEEE Trans. Antennas and Propagation*, **24**, 155–162

Hanel R.A., B. Schlachman, D. Rogers and D. Vanous, 1971, Nimbus-4 Michelson interferometer, *Applied Optics*, **10**, 1376–1382

Houghton J.T., F.W. Taylor and C.D. Rodgers, 1984, *Remote Sounding of Atmospheres*. Cambridge Planetary Science Series, Cambridge University Press

Levi L., 1968, *Applied optics: A guide to modern optical system design*. Wiley, New York

Liou Kuo–Nan, 1980, *An introduction to atmospheric radiation*. Academic Press Inc.

McCartney E., 1983, *Absorption and emission by atmospheric gases: The physical processes*. John Wiley & Sons

Twomey S., 1977, *Introduction to the mathematics of inversion in remote sensing and indirect measurements*. Elsevier Scientific Publishing Company, New York

Valley S.L., 1965, *Handbook of geophysics and space environments*. McGraw–Hill, New York